

Review

Modern Theoretical Approaches to Modeling the Excited-State Intramolecular Proton Transfer: An Overview

Joanna Jankowska ^{1,*}  and Andrzej L. Sobolewski ²¹ Faculty of Chemistry, University of Warsaw, 02-093 Warsaw, Poland² Institute of Physics, Polish Academy of Sciences, 02-668 Warsaw, Poland; sobola@ifpan.edu.pl

* Correspondence: jjankowska@chem.uw.edu.pl

Abstract: The excited-state intramolecular proton transfer (ESIPT) phenomenon is nowadays widely acknowledged to play a crucial role in many photobiological and photochemical processes. It is an extremely fast transformation, often taking place at sub-100 fs timescales. While its experimental characterization can be highly challenging, a rich manifold of theoretical approaches at different levels is nowadays available to support and guide experimental investigations. In this perspective, we summarize the state-of-the-art quantum-chemical methods, as well as molecular- and quantum-dynamics tools successfully applied in ESIPT process studies, focusing on a critical comparison of their specific properties.

Keywords: excited-state intramolecular proton transfer; photochemistry; photobiology; quantum chemistry; molecular dynamics; ultrafast processes



Citation: Jankowska, J.; Sobolewski, A.L. Modern Theoretical Approaches to Modeling the Excited-State Intramolecular Proton Transfer: An Overview. *Molecules* **2021**, *26*, 5140. <https://doi.org/10.3390/molecules26175140>

Academic Editor: Mirosław Jabłoński

Received: 15 July 2021

Accepted: 23 August 2021

Published: 25 August 2021

Publisher's Note: MDPI stays neutral with regard to jurisdictional claims in published maps and institutional affiliations.



Copyright: © 2021 by the authors. Licensee MDPI, Basel, Switzerland. This article is an open access article distributed under the terms and conditions of the Creative Commons Attribution (CC BY) license (<https://creativecommons.org/licenses/by/4.0/>).

1. Introduction

Photochemistry of organic molecular systems is an extremely rich and exciting field of research, continuously growing and, thus, pushing forward the frontiers of our understanding of light–matter interactions. Among many chemical processes induced with photon absorption, the excited-state intramolecular proton transfer (ESIPT) stands out with its ultrashort timescale and strong impact on the molecular electronic structure, which is often manifested with large emission Stokes shifts. Relying on a proton exchange between two electronegative centers along a pre-existing intramolecular hydrogen bond, the ESIPT process is recognized to provide a mechanism of excellent photostability to natural and artificial molecular systems [1–3], finds applications in fluorescent probes and imaging agents [4–6], governs characteristic emission of the green fluorescent protein and its analogs [7–9], and opens rich possibilities for multicolor emission in organic light-emitting diodes (OLEDs) [10–14]. Last but not least, ESIPT may also activate other excited-state reaction channels, facilitating the design of complex molecular photo-devices [15–19].

In its typical arrangement, ESIPT occurs upon photoexcitation of a molecular system including two moieties connected on the one side by an intramolecular hydrogen bond and with an electronically conjugated network of covalent bonds on the other side, as shown in Figure 1. The reaction occurs in an excited electronic state and is usually being parameterized by the distance between the proton-donor (D) atom (most commonly oxygen or nitrogen [15,20,21]) and the transferring proton. The proton-accepting (A) moiety consists of another electronegative center, often including a carbonyl or an imine group [11,17], which, in order for the ESIPT process to be efficient, should exhibit stronger basicity in the excited state than the proton donor. After the proton transfer, the system undergoes further electronic relaxation—either radiative or nonradiative in nature. In the former case, the characteristic strongly red-shifted fluorescence is nowadays regarded as the hallmark of ESIPT. The latter scenario requires the presence of an independent nonradiative deactivation channel, induced, for instance, by a *cis/trans* isomerization reaction [22]. While the ultrafast ESIPT process is often reported to have ballistic nature (that is, barrierless

excited-state potential-energy (PE) landscape in Figure 1), it may also involve passage through an energy barrier or include nonadiabatic transition/intersystem crossing between different electronic states. Similarly, after the relaxation to the ground electronic state, the system may reach a local PT minimum or may undergo a spontaneous back-transfer to the initial D–H bonded isomer. This final reaction-cycle closing transformation is sometimes referred to as a ground-state intramolecular proton transfer (GSIPT).

In the context of the following discussion, it is also important to underline a distinction between the ESIPT reaction investigated herein and similar processes, especially the proton-coupled electron transfer (PCET) reaction [23–26]. The latter phenomenon, often of nonadiabatic character, has a generally much more complex nature and may involve ground and excited-state reactions, such as intra- and intermolecular, concerted, and step-wise processes. Under certain conditions, ESIPT may play the role of an elementary step in a complex PCET reaction.

In this review, we identify and discuss three fundamental families of theoretical approaches to modeling the ESIPT process: (i) the static methods, (ii) the mixed quantum-classical molecular dynamics, and (iii) the quantum dynamics methods. In the following sections, we briefly outline their theoretical assumptions, comment on the scope of their applicability and performance in ESIPT studies, and highlight recent achievements in each field, focusing on the most illustrative results from the last 5 years. For a broader view of ESIPT-focused research, including also experimental insights, the interested reader is referred to other up-to-date reviews [4,6,21,27,28] and monographs [29–32] that have been published on the subject.

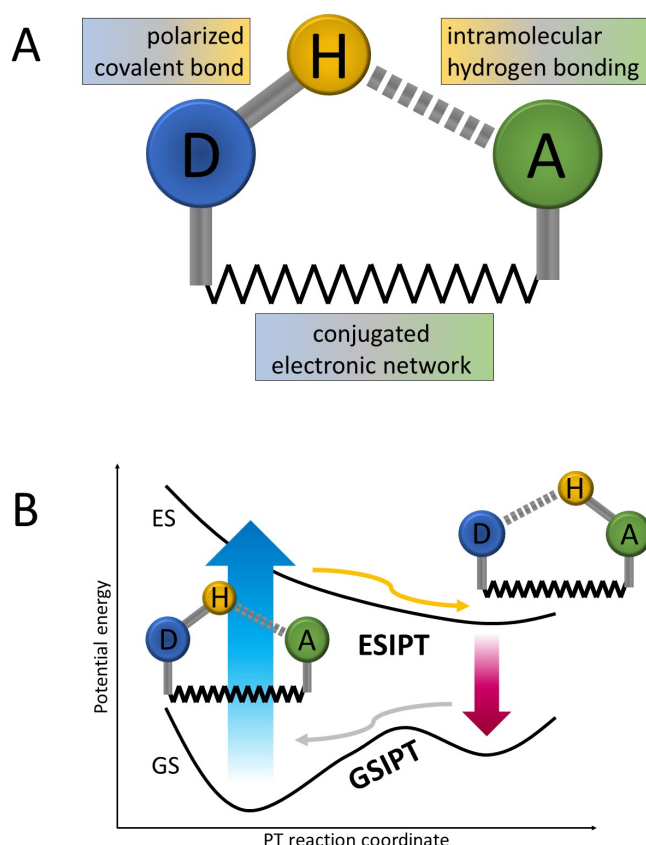


Figure 1. Schematic representation of the ESIPT mechanism: (A) initial atomic arrangement of an ESIPT system; (B) typical (most basic) potential energy landscape along the ESIPT reaction coordinate. D—proton donor; A—proton acceptor; GS—ground electronic state; ES—excited electronic state; blue arrow—initial photoabsorption; red arrow—Stokes-shifted fluorescence.

2. Static Investigation Approach

2.1. Objective of the Static Calculations

The most straightforward approach to the theoretical characterization of a new photochemical system relies on a “static” quantum-chemical investigation, which itself might be a target research strategy or an initial step of a more complex protocol. The static ESIPT investigation is primarily oriented toward providing high-quality absorption and emission optical energies, as well as the topographical description of the investigated system’s PE landscape. It might also be considered a lower-cost computational option for large polyatomic molecules as this protocol, compared to the dynamic ones, usually involves a relatively limited number of demanding energy-gradient calculations and facilitates further savings by allowing calculations under fixed system symmetry, if such is present. Typical outcomes of the static approach are absorption and emission vertical electronic energies [33–36], upper-bound estimations for possible energy barriers in the ground and electronically excited states [36–38], and detailed characterization of these states in terms of symmetry and orbital configuration [38,39]. Moreover, the number of other molecular features complementing the experimental ESIPT characterization can be determined, including, e.g., tautomers relative energies [35,40], atomic charges [41–43], and vibrational modes attribution [44,45].

2.2. Typical Investigation Workflow

A typical workflow scheme of the static protocol is presented in Figure 2. In the first step, a search for stationary points on the ground-state (GS) potential energy surface (PES) is performed, followed by vertical electronic excitation energies calculations. At this stage, the electronic structure of the GS and the character of the relevant excited states (ES) need to be carefully evaluated, with a special focus on expected requirements for the excited-state methods to be applied in the following steps. Afterward, an analysis of ES relaxed properties is conducted, and the barrierless/barrier-restricted character of ESIPT is determined by excited-state geometry optimization of the relevant isomers, along with predictions for the energy and intensity of the Stokes-shifted fluorescence [38,46]. In the final step, adiabatic potential energy profiles (PEPs) [47,48] or PESs [3,33] may be calculated, if one or multiple reaction coordinates, respectively, need to be explicitly considered. In certain cases, the energy profiles of linearly interpolated reaction paths might also efficiently support the static ESIPT analysis [49]. However, in accordance with the static protocol name, it should be stressed that neither dynamic nor kinetic effects beyond the zero-point energy (ZPE) corrections to electronic stationary-point energies are included at this level of theory.

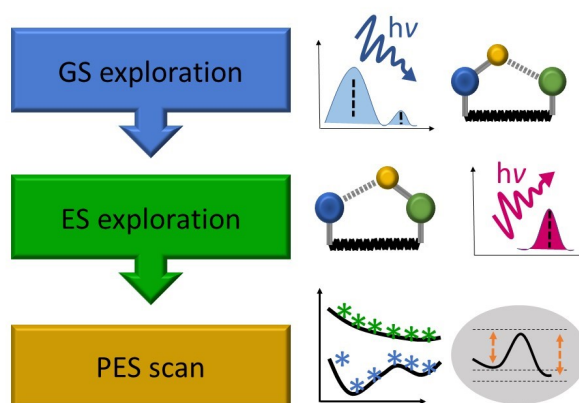


Figure 2. Typical workflow of the static ESIPT investigation protocol.

2.3. Applied Tools and Methods

In principle, the static ESIPT investigation can be performed with any kind of electronic structure method capable of treating the electronic structure of excited states in a relaxed manner. Typically, single-reference electronic structure methods can be trusted to reproduce accurately the topography of the involved electronic states, with the exception of an anti-Kasha ESIPT [50] or systems with low-lying doubly excited states [42,51]. The choice of the optimum electronic structure method for a particular ESIPT study is usually dictated, on the one hand, by the size of the molecular system and, on the other, by its specific electronic structure features. An important general observation is that the correct characterization of the PES topography of the proton-transfer process necessarily requires the inclusion of dynamic electronic correlation effects, as artificial or overestimated reaction barriers have been reported otherwise [52–54].

2.3.1. Ab Initio Wave Function Approaches

For the smaller molecular systems (generally, up to 50 heavy atoms), coupled-cluster electronic structure methods, such as the simplified version of singles and doubles, CC2 [55,56], and the algebraic diagrammatic construction method (ADC(2)) [57,58], have been the methods of choice for a long time [3,34,46,49,59]. The reason is their universality [60] and the availability of well-tested and efficient implementations in widely distributed quantum-chemical software packages. While the CC2 method yields overall slightly more accurate electronic excitation energies [58], the virtue of the ADC(2) approach lies in better numerical stability near-electronic excited-state crossings [61–63].

At the same time, regarding the recent reports of previously unrecognized troubles of the CC2 and ADC(2) methods in predicting accurate excited-state PES beyond the Franck–Condon vicinity [64,65], spin-component scaled CC2 (SCS-CC2 [66]) and scaled opposite spin CC2 (SOS-CC2 [67,68]) approaches have been found particularly promising in the context of ESIPT studies. In this direction, one of us recently employed both these protocols in combination with the ADC(2) method to model photophysical transformations in several salicylaldehyde derivatives [34], observing indeed their improved performance for ESIPT-driven fluorescence energy calculations; similar results have also been reported by Kielesinski et al. for coumarins [69]. In this latter work, performed quantum-chemical investigation yielded correct predictions of solvatochromic effects in a series of compounds, studied both by experimental and theoretical means. Moreover, a direct explanation for single- and multicolor emission observed experimentally in closely related coumarin systems has been formulated on the grounds of a detailed computational analysis of the lowest-energy electronic excited states' properties.

2.3.2. Density Functional Theory Methods

The second widely applied family of electronic structure methods for ESIPT investigations is time-dependent density functional theory (TD-DFT [70]), in its original design and within the Tamm–Dancoff approximation (TDA-DFT [71]). Abundant ESIPT studies at this level of theory [33,40,46,48,72,73] take advantage of the favorable scaling of DFT with the system size. At the same time, due to known difficulties of TD-DFT with the description of charge-transfer states, and more recent findings on its troubles with the proper determination of state orders in inverted singlet/triplet systems [74,75], the choice of the exchange-correlation functional and method validation usually need to be carefully conducted before meaningful conclusions can be formulated [36,59,76].

In recent years, many functionals of different types have been employed in ESIPT studies [59]. In particular, the popular Becke three-parameter Lee–Yang–Parr (B3LYP) [77,78] functional was found to perform well for systems exhibiting small or no charge-transfer effect in the excited states involved in the ESIPT reaction [3,33,37,72,73,76]. Other recently applied and promising functionals include hybrid meta M06-2X [38,40,46,79], and long-range and dispersion-corrected ω B97X-D [40,80,81]. Among other reported possibilities, the Coulomb-attenuated hybrid functional CAM-B3LYP [82] has also recently gained a

relatively trusted position as a tool for ESIPT investigations [36,73,76,81]. At the same time, none of these functional choices appear to be fully universal as of today [59]. As for the TD-DFT relation to TDA-DFT, the latter shows generally higher stability at the interstate crossings, including improved performance in the vicinity of conical intersections [83], even those involving the reference electronic state, and allows for some additional computational-time savings [81,84], appearing particularly attractive in the context of ESIPT dynamics simulations.

Finally, due to known DFT deficiencies in describing dispersion interactions [85], it is worth noting the role of these effects in ESIPT modeling at the TD-DFT level. It is observed that a suitable correction, such as D3 or D4 as proposed by Grimme et al. [86,87] or direct application of a dispersion-corrected functional (e.g., ω B97X-D) is typically required for proper treatment of microsolvated, supramolecular, or condensed-phase (e.g., crystal) systems, in which explicit interactions between the core molecule and the environment have to be included [88–90]. On the other hand, in most other cases, the omission of the dispersion part of interaction energy does not seem to play a significant role, as revealed by the generally good performance of common uncorrected exchange-correlation functionals [59,76].

2.3.3. Basis-Set Choice

Practical application of the methods discussed above requires making the additional choice of a basis set for the wave-function expansion, which has a direct impact on the quality of the results. In this case, again one needs to make a compromise between the computational cost and desired accuracy. Most common recent choices in ESIPT studies seem to be favoring the cc-pVTZ [91] basis set from the Dunning family on the one hand [3,33,39,40,48], and different variants of the Pople 6-311 G(d,p) [92] basis set, on the other [36,72,73]. The latter direction finds its support in a general study by Laurent et al. [93], in which the basis-set effect on vertical excitation energy calculations was investigated. On the grounds of reported results, however, it is not easy to make definite ESIPT-targeted recommendations for the basis-set choice since both system and ES-specific effects come into play [93].

2.3.4. Solvent Effects

Finally, a brief discussion of the environmental effects is appropriate, as ESIPT systems are usually investigated in solution or in other complex condensed-phase environments. In particular, the polarity of the surrounding medium has been observed to have a strong impact on the ESIPT reaction efficiency [73,76].

Thus far, several different approaches have been employed to tackle environmental effects on ESIPT, including microsolvation [43,69], the conductor-like screening model (COSMO) [48,94,95], the polarizable continuum model (PCM) [76,96,97], the solvent model density (SMD) method [46,98], and the integral equation formalism version of PCM (IEF-PCM) [99–101]. The latter approach, particularly popular recently [33,37,73,102], has been applied e.g. by Wang et al. to the BTS system [39] in methylene chloride, yielding very high accuracy predictions for excitation and emission wavelengths, with divergence from the experimental values measured in just a few nm. In addition to the general purpose methods listed above, state-specific PCM treatments of correlated linear response (cLR) [103] and the vertical excitation model within the unrelaxed density approximation (VEM-UD) [104,105] have been successfully applied to study ESIPT by Vérité et al. [40], who pointed out the advantages that these approaches bring for the description of charge-transfer states in ESIPT reactions. Nevertheless, the explicit inclusion of (typically few) solvent molecules is necessary in certain cases, especially for protic solvents and solvents exhibiting proton-accepting properties, since resulting competition between intra- and intermolecular hydrogen bond formation may drastically affect the ESIPT reaction yield [88,90,106].

2.4. Summary of the Static ESIPT Investigation Methods

To summarize the section dedicated to the static ESIPT investigation protocol, we again underline its strengths as being a relatively affordable and yet informative approach, designed to provide a fundamental characterization of ESIPT, including the system's absorption and emission properties, as well as information on the topography of GS and ES PESs over pre-selected reaction coordinates. Due to its inherent compatibility with a great variety of electronic structure methods, this protocol allows researchers to take advantage of new developments in electronic structure theory and, thus, constantly provides opportunities for cutting-edge studies of ESIPT in all types of molecular systems.

At the same time, it should be noted that, under certain circumstances, the investigation of static ESIPT paths may not be sufficient. In particular, systems undergoing multiple PT reactions are typically challenging to be accurately studied with this protocol due to the large computational cost of multi-dimensional PES scans, on the one hand, and the critical role of the sequence of individual processes missed at this level, on the other hand. Another situation, in which special precautions should be taken, is when ESIPT occurs within a dense manifold of electronic states, such as in situations in which a competition between various photochemical transformations is to be expected; in these cases, one may need to explicitly determine the relative efficiency of each channel, which usually requires the inclusion of nuclear-dynamic effects.

3. Nonadiabatic Molecular Dynamic Approaches

New opportunities of delving deeper into the course of the ESIPT reaction open when one turns toward dynamic approaches. In the most general view, this refers to a large (and growing) number of methods allowing for real-time simulations of molecular systems' evolution in terms of their electronic and nuclear structure, beyond the static picture.

The time-dependent Schrödinger equation is the core and starting point for the dynamic methods, yielding two broad families of approaches, differed by the level of the applied approximations. The first family consists of fully quantum dynamic (QD) methods, in which electronic and nuclear degrees of freedom are treated both at the quantum-mechanical level. The second family is built on nonadiabatic mixed quantum–classical (NA-MQC) dynamics methods, in which the nuclei, which are much slower than the electrons, are treated at the classical or semi-classical level, propagating under the Newton equation of motion. The quantum–electronic and classical–nuclear subsystems are in this picture connected by the nonadiabatic coupling, ensuring the self-consistency of the description of the total molecular system. We start our discussion of ESIPT nonadiabatic molecular dynamics studies with the NA-MQC methods, which will be subsequently followed by the analysis of the QD performance, in line with the increasing level of the method exactness.

3.1. Mixed Quantum–Classical Dynamic Calculations in ESIPT Studies

The NA-MQC methods, recently summarized in an excellent review by Crespo-Otero and Barbatti [107], can be divided into several groups, out of which the trajectory surface hopping (TSH) [108–111], ab initio multiple spawning (AIMS) [112,113], and, most recently, the nuclear–electronic orbital Ehrenfest (NEO-Ehrenfest) [114] methods are, to the best of our knowledge, the ones that have been successfully employed in dynamic ESIPT investigations thus far. Below, a brief characterization of these approaches is provided, along with an illustration of their performance for the description of the ESIPT process. Additionally, a schematic representation of their underlying mechanisms is presented in Figure 3.

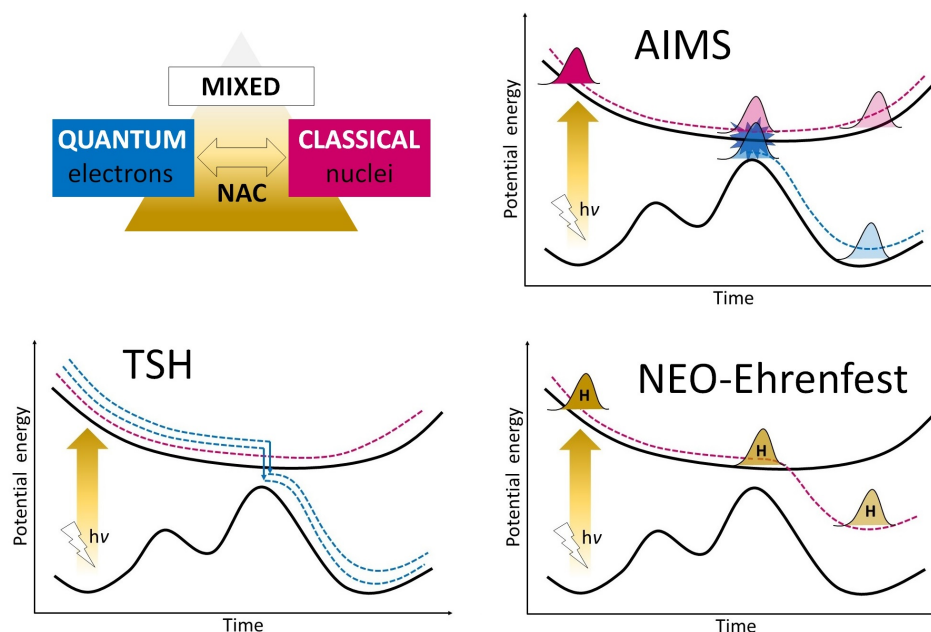


Figure 3. Schematic illustration of the mechanisms of the discussed NA-MQC dynamic approaches: trajectory surface hopping (TSH), ab initio multiple spawning (AIMS), and nuclear–electronic orbital Ehrenfest (NEO-Ehrenfest).

3.1.1. Trajectory Surface Hopping Approach

The trajectory surface hopping method, especially under Tully’s fewest-switches (FSSH) [108] algorithm and under other algorithms based on the Landau–Zener (LZ) model [115,116], is the most widely used NA-MQC approach in ESIPT studies thus far. TSH relies on the modeling of the real-time evolution of the molecular system by a set of independent classical trajectories, which together are assumed to represent a nuclear wave packet in an approximate (statistical) way. While the trajectories are propagated on individual Born–Oppenheimer adiabatic PESs, nonadiabatic transitions between these surfaces are possible in regions characterized by large interstate nonadiabatic couplings (NACs). The interstate transitions are controlled by a stochastic algorithm (FSSH) or induced in minimum-energy-gap regions (LZ methods), with the “hopping” probability proportional to the NAC. Importantly, the TSH method can be implemented as an “on-the-fly” approach [117], which means that the actual PES, on which the system is propagating, does not have to be known in advance, and electronic properties, such as energies or gradients, are calculated along the NA-MQC path as needed. It should be noted, however, that usually, many trajectories are required for reliable and converged TSH results [107].

As of today, the TSH method has been implemented in a number of dedicated software packages, including Newton X [118,119], Shark [120], Jade [121], etc. [107]. In all cases, the NA-MQC dynamics protocol has to be paired with an electronic structure method, and its choice needs to be made with great care, as it directly impacts the quality of the results, as well as the simulation cost. One needs to be aware, however, that due to the inherent mixed-classical nature of the TSH approach, certain effects that may play an important role in the ESIPT reaction cannot be reproduced at the TSH level of theory. This includes all phenomena stemming from the nonlocality of the true nuclear wave function, which is reduced to a single point on adiabatic PES within the TSH picture. In particular, proton tunneling, wave-packet interference, and decoherence effects are not included, the latter being partially restored in the TSH simulations via the introduction of various kinds of decoherence corrections [122].

In terms of recent applications of the TSH methodology to particular ESIPT studies, Li et al. reported interesting results explaining 3-hydroxyflavone dual fluorescence in solvents containing protic contamination with a competition between intra- and intermolecular excited-state PT reactions [90], discussing an effect of the number of explicitly

included water molecules on the simulation outcomes. In this case, the applied FSSH/TD-DFT methodology allowed for high-quality predictions of the electronic excitation energies (typical error below 0.2 eV) and also yielded ESIPT timescale in very good agreement with available experimental data, with a deviation of less than 10 fs. Another challenging aspect of dealing with a large number of possible photo-reaction products has been tackled by Tuna et al., who employed a robust multiconfiguration interaction variant of the orthogonalization-corrected semi-empirical OM2 approach to model ESIPT-driven photochemistry of urocanic acid [123]. The same method has also been applied by Xia et al. to study relaxation mechanisms in the isolated benzodiazepinone molecule, in which several interconnected relaxation channels come to play [124]. Furthermore, we recently performed a TSH study at the TDA-DFT level to analyze the impact of the character of the lowest excited state on the ESIPT process efficiency [84], eventually confirming the important role of the $\pi\pi^*$ states.

3.1.2. Ab Initio Multiple Spawning Approach

Another NA-MQC approach that has found applications in time-resolved ESIPT simulations is the ab initio multiple spawning method. AIMS originates from the formally exact full multiple spawning methodology [125,126]. Its core concept relies on representing the nuclear wave function with partially coupled traveling Gaussian functions, having a finite width both in position and momentum coordinates and interacting during the dynamics. Importantly, the total number of the “on-the-fly” propagated Gaussian functions changes in time since on each passage through a PES region characterized with strong NAC, a new Gaussian is spawned (hence, the S in AIMS).

Similar to the TSH case, AIMS simulations require combining the particular MS protocol with a suitable electronic structure method. As for the AIMS code itself, as of today, it is available within several software packages, including GAMESS [127,128], MOLPRO [129,130], and MOPAC [131,132]. Technically, AIMS involves a higher computational cost than TSH, yet it should be considered a superior approach, inherently including decoherence effects, and yielding a correct description of some non-local phenomena. At the same time, due to certain intrinsic limitations of the AIMS approach, the tunneling effect, although theoretically possible to be covered through the intrastate spawning procedure [112,125], is not reproduced at this level of theory [113].

Turning to recent interesting applications of the AIMS in ESIPT studies, Pijeu et al. investigated the photophysics of the paradigmatic salicylideneaniline (SA) system [133], focusing on the effect of nonplanarity on ESIPT and on the total deactivation mechanism. In this study, the AIMS protocol has been connected with the floating occupation molecular orbital complete active space configuration interaction (FOMO-CASCI) method, with further wave function-in-DFT embedding. The same group also tackled the hydroxyphenyl benzothiazole (HBT) system at this level of theory, obtaining very good agreement with the experimental results [134].

3.1.3. Nuclear–Electronic Orbital Ehrenfest Approach

Recently, a new NA-MQC dynamic approach, NEO-Ehrenfest, aiming toward the further enhanced recovery of nonlocal effects, has been developed. Within this method, protons are treated quantum mechanically on an equal footing with the electrons, yielding automatic inclusion of the ZPE, quantized vibrational levels, and tunneling effects associated with these species [114]. The NEO-Ehrenfest approach, specifically tailored to provide a high-level description of the ESIPT and PCET processes [135], is built on the concept of semi-classical traveling proton basis functions, which, on the one hand, provide means for the quantum-mechanical representation of protons, as has been demonstrated before for the time-independent case [136], and, on the other hand, enable the description of its long-range displacements.

In a recent pioneering NEO-Ehrenfest study by Zhao et al. the ESIPT process in o-hydroxy-benzaldehyde has been investigated [135]. Upon comparison of results obtained

using the NEO-Ehrenfest and the traditional Ehrenfest approach [137] with all-classical nuclei, the proton transfer reaction acceleration in the quantum case has been observed, which has been ascribed to the delocalization of the proton wave function, resulting in a smaller necessary displacement of the proton-accepting and proton-donating centers. Moreover, the kinetic isotope effect upon deuterium substitution has been reproduced at this level of theory.

3.1.4. Summary of the NA-MQC Dynamic ESIPT Simulations

To summarize the section dedicated to mixed quantum–classical ESIPT studies, we again highlight the great contributions of the NA-MQC dynamic methods for the field. By allowing real-time picturing of the proton transfer process, characteristic timescales and unforeseen reaction mechanisms can be modeled at this level of theoretical description. While the methods share the mixed quantum–classical nature, they also still bear important differences, making them possible methods of choice for different conditions. In particular, TSH is a robust and probably most universal tool, reliable for the modeling of barrierless ESIPT, including complex situations, in which multiple PTs or competition from other photoreaction channels needs to be taken into account. The AIMS approach, formally more exact, may also be generally applied to this class of processes, as long as it does not become prohibitively expensive due to the extended molecular system size. At the same time, when nuclear quantum effects of protons are expected to play a role, such as in the barrier-restricted ESIPT case, the NEO-Ehrenfest method may be considered a good choice.

3.2. Quantum Dynamics Methods for ESIPT Simulations

Despite many useful conclusions on the ESIPT reaction course that may be taken from the NA-MQC dynamics, there are situations in which one needs to advance even further with the level of the system's dynamic description, up to the point of full quantum treatment of all the species, including nuclei. As has been already pointed out, the most typical reason of adopting this approach is when tunneling through an energy barrier along the ESIPT path needs to be included, i.e., when highly accurate rates or proton-transfer equilibrium have to be characterized. Another situation calling for the QD treatment is when a strongly nonadiabatic ESIPT mechanism is expected, e.g., when trivial interstate crossings are present, potentially threatening the correct NA-MQC dynamics performance. The latter problem, however, has been, in recent years, partially resolved by the successful design of correction strategies to several NA-MQC protocols [138–140].

Multiconfiguration Time-Dependent Hartree Method

Among the most robust approaches to solving the time-dependent Schrödinger equation that retain the quantum character of all the molecular system's components, the multiconfiguration time-dependent Hartree (MCTDH) method plays, up to date, the most prominent role [141]. Relying on the Born–Huang expansion, the MCTDH allows for propagating a wave-packet in time with the wave function of the system represented by the sum of products of so-called single-particle functions describing individual nuclear degrees of freedom (DOF), which are typically associated with the molecular normal vibrational modes. The MCTDH method employs model Hamiltonians, constructed individually for each system. In the case of the ESIPT studies, usually, a vibronic Hamiltonian is employed [142–144], including a pre-selected number of electronic PESs and nuclear DOFs. It should be noted that MCTDH requires the determination of the PESs prior to the MCTDH calculation. This is typically achieved by combining quantum-chemical probing of the PES regions expected to play the most important role in the investigated process with the application of various interpolation models to approximate the remaining PES areas.

In practical terms, the original MCTDH method can nowadays cover in a general case up to ca. 20 DOFs, but in recent years, new flavors of MCTDH have been developed, such as the multilayer multiconfiguration time-dependent Hartree (ML-MCTDH) method, which pushes this limit even up to several thousand DOFs [145]. The performance boost

stems, in this case, from a tree-like (layered) representation of the nuclear wave function, in which the traditional SPFs are further expanded themselves in the MCTDH spirit. The eventual efficiency gain, however, depends strongly on the system's nature and size [145]. As of today, different variants of the MCTDHF methods are available in a few dedicated software packages, such as the Heidelberg MCTDH [146], or Quantics [147].

Moving to the MCTDHF applications to simulating the ESIPT process, interesting results on the photophysics of hydroxychromones have been reported by Perveaux et al. [148] and Anand et al. [149]. In the former case, the full-dimensional (48 DOFs) ML-MCTDH method was applied to analyze the interplay between the ESIPT reaction and the out-of-plane hydrogen torsion in 3-hydroxychromone, while the latter study comprised analogical simulations for the 3-hydroxychromone and 5-hydroxychromone systems, performed at the multimode MCTDH level with the inclusion of 25 DOFs. Both investigations led to similar conclusions on a critical role of a conical intersection between bright S_1 and dark S_2 states, of respective $\pi\pi^*$ and $n\pi^*$ character, which was interpreted as the reason for observation of two ESIPT rate constants for these molecules in the experiment. Anand et al. applied the same methodology to study ESIPT also in similar 3-hydroxyflavone [150] and 3-hydroxypyran-4-one [151] systems, confirming the important role of the S_2 state in their photorelaxation. Finally, recent thorough work by Cao et al. provided theoretical insights on ESIPT-driven mechanism and quantum dynamics of thermally activated delayed fluorescence in triquinolonobenzene [152], in which singlet-state ultrafast proton transfer occurs within a dense manifold of low-lying triplet states.

4. Summary and Future Outlook

In summary, in the present review, we gathered and discussed key features of the modern theoretical approaches employed in ESIPT investigations, with a special focus on their complementary capabilities and critical limitations. Depending on the particular research focus, e.g., manifested by the need for detailed knowledge of ES topography, equilibrium populations of different molecular isomers, or characterization of time-resolved effects, and the system-specific challenges, such as the isolated or band-like arrangement of the active excited states, presence of barrier-restricted or barrierless PT, the necessity of taking the intersystem crossing into account, etc., a proper theoretical approach in each case can be proposed. To this end, we hope that this sometimes challenging choice will be facilitated with the provided insights.

Looking toward future developments that would further strengthen the field, support from machine learning techniques should definitely be considered a promising direction for the QD efficiency enhancement, with first results already emerging [153,154], so as to improve the performance of other dynamic approaches [155]. Moreover, linking solvent-dependent optical properties with nonadiabatic ESIPT dynamics within the fully quantum framework could also provide powerful new tool to the existing set [151], opening new-level possibilities, e.g., for describing the competition between intra- and intermolecular excited-state proton transfer reactions on equal footing.

Funding: This research received no external funding.

Institutional Review Board Statement: Not applicable.

Informed Consent Statement: Not applicable.

Data Availability Statement: All data are available within the article and the included references.

Acknowledgments: The Authors would both like to thank Wolfgang Domcke for the great support and fruitful discussion on the preparation of the manuscript.

Conflicts of Interest: The authors declare no conflict of interest.

References

1. Gong, Y.; Wang, Z.; Zhang, S.; Luo, Z.; Gao, F.; Li, H. New ESIPT-inspired photostabilizers of two-photon absorption coumarin–benzotriazole dyads: From experiments to molecular modeling. *Ind. Eng. Chem.* **2016**, *55*, 5223–5230. [[CrossRef](#)]
2. Maity, S.; Chatterjee, A.; Chakraborty, N.; Ganguly, J. A dynamic sugar based bio-inspired, self-healing hydrogel exhibiting ESIPT. *New J. Chem.* **2018**, *42*, 5946–5954. [[CrossRef](#)]
3. Berenbeim, J.A.; Boldissar, S.; Owens, S.; Haggmark, M.R.; Gate, G.; Siouri, F.M.; Cohen, T.; Rode, M.F.; Schmidt Patterson, C.; De Vries, M.S. Excited state intramolecular proton transfer in hydroxyanthraquinones: Toward predicting fading of organic red colorants in art. *Sci. Adv.* **2019**, *5*, eaaw5227. [[CrossRef](#)]
4. Sedgwick, A.C.; Wu, L.; Han, H.H.; Bull, S.D.; He, X.P.; James, T.D.; Sessler, J.L.; Tang, B.Z.; Tian, H.; Yoon, J. Excited-state intramolecular proton-transfer (ESIPT) based fluorescence sensors and imaging agents. *Chem. Soc. Rev.* **2018**, *47*, 8842–8880. [[CrossRef](#)] [[PubMed](#)]
5. Long, R.; Tang, C.; Xu, J.; Li, T.; Tong, C.; Guo, Y.; Shi, S.; Wang, D. Novel natural myricetin with AIE and ESIPT characteristics for selective detection and imaging of superoxide anions in vitro and in vivo. *Chem. Comm.* **2019**, *55*, 10912–10915. [[CrossRef](#)]
6. Li, Y.; Dahal, D.; Abeywickrama, C.S.; Pang, Y. Progress in tuning emission of the excited-state intramolecular proton transfer (ESIPT)-based fluorescent probes. *ACS Omega* **2021**, *6*, 6547–6553. [[CrossRef](#)]
7. Hsieh, C.C.; Chou, P.T.; Shih, C.W.; Chuang, W.T.; Chung, M.W.; Lee, J.; Joo, T. Comprehensive studies on an overall proton transfer cycle of the ortho-green fluorescent protein chromophore. *JACS* **2011**, *133*, 2932–2943. [[CrossRef](#)] [[PubMed](#)]
8. Vegh, R.B.; Bloch, D.A.; Bommarius, A.S.; Verkhovsky, M.; Pletnev, S.; Iwai, H.; Bochenkova, A.V.; Solntsev, K.M. Hidden photoinduced reactivity of the blue fluorescent protein mKalama1. *Phys. Chem. Chem. Phys.* **2015**, *17*, 12472–12485. [[CrossRef](#)]
9. Chatterjee, T.; Lacombat, F.; Yadav, D.; Mandal, M.; Plaza, P.; Espagne, A.; Mandal, P.K. Ultrafast dynamics of a green fluorescent protein chromophore analogue: Competition between excited-state proton transfer and torsional relaxation. *J. Phys. Chem. B* **2016**, *5*, 9716–9722 [[CrossRef](#)]
10. Tang, K.C.; Chang, M.J.; Lin, T.Y.; Pan, H.A.; Fang, T.C.; Chen, K.Y.; Hung, W.Y.; Hsu, Y.H.; Chou, P.T. Fine tuning the energetics of excited-state intramolecular proton transfer (ESIPT): White light generation in a single ESIPT system. *JACS* **2011**, *133*, 17738–17745. [[CrossRef](#)]
11. Wu, K.; Zhang, T.; Wang, Z.; Wang, L.; Zhan, L.; Gong, S.; Zhong, C.; Lu, Z.H.; Zhang, S.; Yang, C. De novo design of excited-state intramolecular proton transfer emitters via a thermally activated delayed fluorescence channel. *JACS* **2018**, *140*, 8877–8886. [[CrossRef](#)]
12. Duarte, L.G.T.A.; Germino, J.C.; Berbigier, J.F.; Barboza, C.A.; Faleiros, M.M.; de Alencar Simoni, D.; Galante, M.T.; de Holanda, M.S.; Rodembusch, F.S.; Atvars, T.D.Z. White-light generation from all-solution-processed OLEDs using a benzothiazole–salophen derivative reactive to the ESIPT process. *Phys. Chem. Chem. Phys.* **2019**, *21*, 1172–1182. [[CrossRef](#)]
13. Czernel, G.; Budziak, I.; Oniszczyk, A.; Karcz, D.; Pustuła, K.; Górecki, A.; Matwijczuk, A.; Gładyszewska, B.; Gagoś, M.; Niewiadomy, A.; et al. ESIPT-related origin of dual fluorescence in the selected model 1,3,4-thiadiazole derivatives. *Molecules* **2020**, *25*, 4168. [[CrossRef](#)]
14. Trannoy, V.; Léaustic, A.; Gadan, S.; Guillot, R.; Allain, C.; Clavier, G.; Mazerat, S.; Geffroy, B.; Yu, P. A highly efficient solution and solid state ESIPT fluorophore and its OLED application. *New J. Chem.* **2021**, *45*, 3014–3021. [[CrossRef](#)]
15. Rode, M.F.; Sobolewski, A.L. Effect of chemical substituents on the energetical landscape of a molecular photoswitch: An ab initio study. *J. Phys. Chem. A* **2010**, *114*, 11879–11889. [[CrossRef](#)]
16. Jankowska, J.; Rode, M.F.; Sadlej, J.; Sobolewski, A.L. Photophysics of Schiff bases: Theoretical study of salicylidene methylamine. *ChemPhysChem* **2012**, *13*, 4287–4294. [[CrossRef](#)] [[PubMed](#)]
17. Böhnke, H.; Bahrenburg, J.; Ma, X.; Röttger, K.; Näther, C.; Rode, M.F.; Sobolewski, A.L.; Temps, F. Ultrafast dynamics of the ESIPT photoswitch N-(3-pyridinyl)-2-pyridinecarboxamide. *Phys. Chem. Chem. Phys.* **2018**, *20*, 2646–2655. [[CrossRef](#)] [[PubMed](#)]
18. Georgiev, A.; Todorov, P.; Dimov, D. Excited state proton transfer and E/Z photoswitching performance of 2-hydroxy-1-naphthalene and 1-naphthalene 5,5'-dimethyl- and 5,5'-diphenylhydantoin Schiff bases. *J. Photochem. Photobiol. A* **2020**, *386*, 112143. [[CrossRef](#)]
19. Huang, A.; Hu, J.; Han, M.; Wang, K.; Xia, J.L.; Song, J.; Fu, X.; Chang, K.; Deng, X.; Liu, S.; et al. Tunable photocontrolled motions of anil-poly(ethylene terephthalate) systems through excited-state intramolecular proton transfer and trans–cis isomerization. *Adv. Mater.* **2021**, *33*, 2005249. [[CrossRef](#)]
20. Hsieh, C.C.; Jiang, C.M.; Chou, P.T. Recent experimental advances on excited-state intramolecular proton coupled electron transfer reaction. *Acc. Chem. Res.* **2010**, *43*, 1364–1374. [[CrossRef](#)]
21. Joshi, H.C.; Antonov, L. Excited-state intramolecular proton transfer: A short introductory review. *Molecules* **2021**, *26*, 1475. [[CrossRef](#)]
22. Sobolewski, A.L.; Domcke, W. Photophysics of intramolecularly hydrogen-bonded aromatic systems: Ab initio exploration of the excited-state deactivation mechanisms of salicylic acid. *Phys. Chem. Chem. Phys.* **2006**, *8*, 3410. [[CrossRef](#)]
23. Hammes-Schiffer, S. Theory of proton-coupled electron transfer in energy conversion processes. *Acc. Chem. Res.* **2009**, *42*, 1881–1889. [[CrossRef](#)]
24. Weinberg, D.R.; Gagliardi, C.J.; Hull, J.F.; Murphy, C.F.; Kent, C.A.; Westlake, B.C.; Paul, A.; Ess, D.H.; McCafferty, D.G.; Meyer, T.J. Proton-coupled electron transfer. *Chem. Rev.* **2012**, *112*, 4016–4093. [[CrossRef](#)] [[PubMed](#)]

25. Domcke, W.; Sobolewski, A.L.; Schlenker, C.W. Photooxidation of water with heptazine-based molecular photocatalysts: Insights from spectroscopy and computational chemistry. *J. Chem. Phys.* **2020**, *153*, 100902. [CrossRef]
26. Tyburski, R.; Liu, T.; Glover, S.D.; Hammarström, L. Proton-coupled electron transfer guidelines, fair and square. *JACS* **2021**, *143*, 560–576. [CrossRef]
27. Serdiuk, I.E.; Roshal, A.D. Exploring double proton transfer: A review on photochemical features of compounds with two proton-transfer sites. *Dyes Pigm.* **2017**, *138*, 223–244. [CrossRef]
28. Chen, L.; Fu, P.Y.; Wang, H.P.; Pan, M. Excited-state intramolecular proton transfer (ESIPT) for optical sensing in solid state. *Adv. Opt. Mater.* **2021**, *52*, 2001952. [CrossRef]
29. Demeter, A. Hydrogen bond basicity in the excited state: Concept and applications. In *Hydrogen Bonding and Transfer in the Excited State*; John Wiley & Sons, Ltd.: Hoboken, NJ, USA, 2010; Chapter 3, pp. 39–78. [CrossRef]
30. Tomin, V.I. Proton transfer reactions in the excited electronic state. In *Hydrogen Bonding and Transfer in the Excited State*; John Wiley & Sons, Ltd.: Hoboken, NJ, USA, 2010; Chapter 22, pp. 463–523. [CrossRef]
31. Stasyuk, A.J.; Solá, M. Excited state intramolecular proton transfer (ESIPT) process: A brief overview of computational aspects, conformational changes, polymorphism, and solvent effects. In *Theoretical and Quantum Chemistry at the Dawn of the 21st Century*; Taylor & Francis Group: London, UK, 2018; Chapter 24. Available online: <https://www.taylorfrancis.com/books/edit/10.1201/9781351170963/theoretical-quantum-chemistry-dawn-21st-century-tanmoy-chakraborty-ramon-carbo-dorca> (accessed on 3 July 2021). [CrossRef]
32. Tang, Z.; Wang, Y.; Zhao, N. Theoretical investigation of excited-state intramolecular proton transfer mechanism of flavonoid derivatives. In *Hydrogen-Bonding Research in Photochemistry, Photobiology, and Optoelectronic Materials*; World Scientific Publishing Co. Pte. Ltd.: Singapore, 2019; Chapter 8, pp. 179–213. Available online: https://www.worldscientific.com/doi/pdf/10.1142/9781786346087_0008 (accessed on 5 July 2021). [CrossRef]
33. Zhang, M.; Zhou, Q.; Du, C.; Ding, Y.; Song, P. Detailed theoretical investigation on ESIPT process of pigment yellow 101. *RSC Adv.* **2016**, *6*, 59389–59394. [CrossRef]
34. Barboza, C.A.; Gawrys, P.; Banasiewicz, M.; Suwinska, K.; Sobolewski, A.L. Photophysical transformations induced by chemical substitution to salicylaldimines. *Phys. Chem. Chem. Phys.* **2020**, *22*, 6698–6705. [CrossRef]
35. Barboza, C.A.; Gawrys, P.; Banasiewicz, M.; Kozankiewicz, B.; Sobolewski, A.L. Substituent effects on the photophysical properties of tris(salicylideneanilines). *Phys. Chem. Chem. Phys.* **2021**, *23*, 1156–1164. [CrossRef]
36. Liang, X.; Fang, H. Theoretical insights into the directionality of ESIPT behavior of BTHMB molecule with two proton acceptors in solution. *Chem. Phys. Lett.* **2021**, *775*, 138670. [CrossRef]
37. Wang, L.; Wang, Y.; Zhang, Q.; Zhao, J. Theoretical exploration about the ESIPT mechanism and hydrogen bonding interaction for 2-(3,5-dichloro-2-hydroxy-phenyl)-benzoxazole-6-carboxylic acid. *J. Phys. Org. Chem.* **2020**, *33*, e4020. [CrossRef]
38. Liu, Z.Y.; Hu, J.W.; Huang, T.H.; Chen, K.Y.; Chou, P.T. Excited-state intramolecular proton transfer in the kinetic-control regime. *Phys. Chem. Chem. Phys.* **2020**, *22*, 22271–22278. [CrossRef] [PubMed]
39. Wang, J.; Liu, Q.; Yang, D. Theoretical insights into excited-state hydrogen bonding effects and intramolecular proton transfer (ESIPT) mechanism for BTS system. *Sci. Rep.* **2020**, *10*, 5119. [CrossRef]
40. Vérité, P.M.; Guido, C.A.; Jacquemin, D. First-principles investigation of the double ESIPT process in a thiophene-based dye. *Phys. Chem. Chem. Phys.* **2019**, *21*, 2307–2317. [CrossRef]
41. Tsai, H.H.G.; Sun, H.L.S.; Tan, C.J. TD-DFT Study of the Excited-State Potential Energy Surfaces of 2-(2'-Hydroxyphenyl) benzimidazole and its Amino Derivatives. *J. Phys. Chem. A* **2010**, *114*, 4065–4079. [CrossRef]
42. Houari, Y.; Chibani, S.; Jacquemin, D.; Laurent, A.D. TD-DFT assessment of the excited state intramolecular proton transfer in hydroxyphenylbenzimidazole (HBI) dyes. *J. Phys. Chem. B* **2015**, *119*, 2180–2192. [CrossRef]
43. Ramu, Y.L.; Jagadeesha, K.; Shivalingaswamy, T.; Ramegowda, M. Microsolvation, hydrogen bond dynamics and excited state hydrogen atom transfer mechanism of 2',4'-dihydroxychalcone. *Chem. Phys. Lett.* **2020**, *739*, 137030. [CrossRef]
44. Zhao, G.J.; Han, K.L. Hydrogen bonding in the electronic excited state. *Acc. Chem. Res.* **2012**, *45*, 404–413. [CrossRef]
45. De Carvalho, F.; Coutinho Neto, M.; Bartoloni, F.; Homem-de Mello, P. Density Functional Theory Applied to Excited State Intramolecular Proton Transfer in Imidazole-, Oxazole-, and Thiazole-Based Systems. *Molecules* **2018**, *23*, 1231. [CrossRef]
46. Chrayteh, A.; Ewels, C.; Jacquemin, D. Dual fluorescence in strap ESIPT systems: A theoretical study. *Phys. Chem. Chem. Phys.* **2020**, *22*, 854–863. [CrossRef]
47. Wu, D.; Guo, W.W.; Liu, X.Y.; Cui, G. Excited-state intramolecular proton transfer in a blue fluorescence chromophore induces dual emission. *ChemPhysChem* **2016**, *17*, 2340–2347. [CrossRef]
48. Vivas, M.G.; Germino, J.C.; Barboza, C.A.; Simoni, D.D.A.; Vazquez, P.A.; De Boni, L.; Atvars, T.D.; Mendonça, C.R. Revealing the dynamic of excited state proton transfer of a π -conjugated salicylidene compound: An experimental and theoretical study. *J. Phys. Chem. C* **2017**, *121*, 1283–1290. [CrossRef]
49. Chaiwongwattana, S.; Škalamera, D.; Došlić, N.; Bohne, C.; Basarić, N. Substitution pattern on anthrol carbaldehydes: Excited state intramolecular proton transfer (ESIPT) with a lack of phototautomer fluorescence. *Phys. Chem. Chem. Phys.* **2017**, *19*, 28439–28449. [CrossRef]
50. Demchenko, A.P.; Tomin, V.I.; Chou, P.T. Breaking the Kasha Rule for More Efficient Photochemistry. *Chem. Rev.* **2017**, *117*, 13353–13381. [CrossRef] [PubMed]

51. Coe, J.D.; Martínez, T.J. Ab initio molecular dynamics of excited-state intramolecular proton transfer around a three-state conical intersection in malonaldehyde. *J. Phys. Chem. A* **2006**, *110*, 618–630. [[CrossRef](#)] [[PubMed](#)]
52. Sobolewski, A.L.; Domcke, W. Ab initio potential-energy functions for excited state intramolecular proton transfer: A comparative study of o-hydroxybenzaldehyde, salicylic acid and 7-hydroxy-1-indanone. *Phys. Chem. Chem. Phys.* **1999**, *1*, 3065–3072. [[CrossRef](#)]
53. Cembran, A.; Gao, J. Excited state intramolecular proton transfer in 1-(trifluoroacetyl-amino) naphthaquinone: A CASPT2//CAS-SCF computational study. *Mol. Phys.* **2006**, *104*, 943–955. [[CrossRef](#)]
54. Li, Y.; Wang, L.; Guo, X.; Zhang, J. A CAS-SCF/CASPT2 insight into excited-state intramolecular proton transfer of four imidazole derivatives. *J. Comput. Chem.* **2015**, *36*, 2374–2380. [[CrossRef](#)]
55. Hättig, C.; Weigend, F. CC2 Excitation Energy Calculations on Large Molecules Using the Resolution of the Identity Approximation. *J. Chem. Phys.* **2000**, *113*, 5154–5161. [[CrossRef](#)]
56. Hättig, C. Geometry optimizations with the coupled-cluster model CC2 using the resolution-of-the-identity approximation. *J. Chem. Phys.* **2003**, *118*, 7751–7761. [[CrossRef](#)]
57. Schirmer, J.; Trofimov, A.B. Intermediate state representation approach to physical properties of electronically excited molecules. *J. Chem. Phys.* **2004**, *120*, 11449–11464. [[CrossRef](#)]
58. Dreuw, A.; Wormit, M. The algebraic diagrammatic construction scheme for the polarization propagator for the calculation of excited states. *WIREs Comput. Mol. Sci.* **2015**, *5*, 82–95. [[CrossRef](#)]
59. Louant, O.; Champagne, B.; Liégeois, V. Investigation of the Electronic Excited-State Equilibrium Geometries of Three Molecules Undergoing ESIPT: A RI-CC2 and TDDFT Study. *J. Phys. Chem. A* **2018**, *122*, 972–984. [[CrossRef](#)] [[PubMed](#)]
60. Jacquemin, D.; Duchemin, I.; Blase, X. 0–0 Energies Using Hybrid Schemes: Benchmarks of TD-DFT, CIS(D), ADC(2), CC2, and BSE/GW formalisms for 80 Real-Life Compounds. *J. Chem. Theory Comput.* **2015**, *11*, 5340–5359. [[CrossRef](#)]
61. Hättig, C. Structure optimizations for excited states with correlated second-order methods: CC2 and ADC(2). *Adv. Quantum Chem.* **2005**, *50*, 37–60. [[CrossRef](#)]
62. Plasser, F.; Crespo-Otero, R.; Pederzoli, M.; Pittner, J.; Lischka, H.; Barbatti, M. Surface hopping dynamics with correlated single-reference methods: 9H-adenine as a case study. *J. Chem. Theory Comput.* **2014**, *10*, 1395–1405. [[CrossRef](#)]
63. Tuna, D.; Lefrançois, D.; Wolański, Ł.; Gozem, S.; Schapiro, I.; Andruniów, T.; Dreuw, A.; Olivucci, M. Assessment of approximate coupled-cluster and algebraic-diagrammatic-construction methods for ground- and excited-state reaction paths and the conical-intersection seam of a retinal-chromophore model. *J. Chem. Theory Comput.* **2015**, *11*, 5758–5781. [[CrossRef](#)]
64. Tajti, A.; Stanton, J.F.; Matthews, D.A.; Szalay, P.G. Accuracy of coupled cluster excited state potential energy surfaces. *J. Chem. Theory Comput.* **2018**, *14*, 5859–5869. [[CrossRef](#)]
65. Tajti, A.; Tulipán, L.; Szalay, P.G. Accuracy of spin-component scaled ADC(2) excitation energies and potential energy surfaces. *J. Chem. Theory Comput.* **2020**, *16*, 468–474. [[CrossRef](#)]
66. Hellweg, A.; Grün, S.A.; Hättig, C. Benchmarking the performance of spin-component scaled CC2 in ground and electronically excited states. *Phys. Chem. Chem. Phys.* **2008**, *10*, 4119. [[CrossRef](#)]
67. Grimme, S. Improved second-order Møller-Plesset perturbation theory by separate scaling of parallel- and antiparallel-spin pair correlation energies. *J. Chem. Phys.* **2003**, *118*, 9095–9102. [[CrossRef](#)]
68. Jung, Y.; Lochan, R.C.; Dutoi, A.D.; Head-Gordon, M. Scaled opposite-spin second order Moller-Plesset correlation energy: An economical electronic structure method. *J. Chem. Phys.* **2004**, *121*, 9793–9802. [[CrossRef](#)]
69. Kielesiński, Ł.; Morawski, O.W.; Barboza, C.A.; Gryko, D.T. Polarized helical coumarins: [1,5] sigmatropic rearrangement and excited-state intramolecular proton transfer. *J. Org. Chem.* **2021**, *86*, 6148–6159. [[CrossRef](#)]
70. Li, T.C.; Tong, P.Q. Time-dependent density-functional theory for multicomponent systems. *Phys. Rev. A* **1986**, *34*, 529–532. [[CrossRef](#)]
71. Hirata, S.; Head-Gordon, M. Time-dependent density functional theory within the Tamm–Dancoff approximation. *Chem. Phys. Lett.* **1999**, *314*, 291–299. [[CrossRef](#)]
72. Sun, C.; Li, H.; Yin, H.; Li, Y.; Shi, Y. Effects of the cyano substitution at different positions on the ESIPT properties of alizarin: A DFT/TD-DFT investigation. *J. Mol. Liq.* **2018**, *269*, 650–656. [[CrossRef](#)]
73. Muriel, W.A.; Morales-Cueto, R.; Rodríguez-Córdoba, W. Unravelling the solvent polarity effect on the excited state intramolecular proton transfer mechanism of the 1- and 2-salicylideneanthrylamine. A TD-DFT case study. *Phys. Chem. Chem. Phys.* **2019**, *21*, 915–928. [[CrossRef](#)]
74. Ehrmaier, J.; Rabe, E.J.; Pristash, S.R.; Corp, K.L.; Schlenker, C.W.; Sobolewski, A.L.; Domcke, W. Singlet–triplet inversion in heptazine and in polymeric carbon nitrides. *J. Phys. Chem. A* **2019**, *123*, 8099–8108. [[CrossRef](#)]
75. De Silva, P. Inverted singlet–triplet gaps and their relevance to thermally activated delayed fluorescence. *J. Phys. Chem. Lett.* **2019**, *10*, 5674–5679. [[CrossRef](#)]
76. Savarese, M.; Raucci, U.; Fukuda, R.; Adamo, C.; Ehara, M.; Rega, N.; Ciofini, I. Comparing the performance of TD-DFT and SAC-CI methods in the description of excited states potential energy surfaces: An excited state proton transfer reaction as case study. *J. Comput. Chem.* **2017**, *38*, 1084–1092. [[CrossRef](#)]
77. Lee, C.; Yang, W.; Parr, R.G. Development of the Colle-Salvetti correlation-energy formula into a functional of the electron density. *Phys. Rev. B* **1988**, *37*, 785–789. [[CrossRef](#)]
78. Becke, A.D. Density-functional thermochemistry. III. The role of exact exchange. *J. Chem. Phys.* **1993**, *98*, 5648–5652. [[CrossRef](#)]

79. Zhao, Y.; Truhlar, D.G. The M06 suite of density functionals for main group thermochemistry, thermochemical kinetics, noncovalent interactions, excited states, and transition elements: Two new functionals and systematic testing of four M06-class functionals and 12 other function. *Theor. Chem. Acc.* **2008**, *120*, 215–241. [[CrossRef](#)]
80. Chai, J.D.; Head-Gordon, M. Long-range corrected hybrid density functionals with damped atom–atom dispersion corrections. *Phys. Chem. Chem. Phys.* **2008**, *10*, 6615. [[CrossRef](#)]
81. Tasheh, N.S.; Nkungli, N.K.; Ghogomu, J.N. A DFT and TD-DFT study of ESIPT-mediated NLO switching and UV absorption by 2-(2'-hydroxy-5'-methylphenyl)benzotriazole. *Theor. Chem. Acc.* **2019**, *138*, 100. [[CrossRef](#)]
82. Yanai, T.; Tew, D.P.; Handy, N.C. A new hybrid exchange–correlation functional using the Coulomb-attenuating method (CAM-B3LYP). *Chem. Phys. Lett.* **2004**, *393*, 51–57. [[CrossRef](#)]
83. Domcke, W.; Yarkony, D.R.; Köppel, H. *Conical Intersections*; World Scientific Publishing Co. Pte. Ltd.: Singapore, 2004. [[CrossRef](#)]
84. Jankowska, J.; Barbatti, M.; Sadlej, J.; Sobolewski, A.L. Tailoring the Schiff base photoswitching—a non-adiabatic molecular dynamics study of substituent effect on excited state proton transfer. *Phys. Chem. Chem. Phys.* **2017**, *19*, 5318–5325. [[CrossRef](#)]
85. Grimme, S. Density functional theory with London dispersion corrections. *WIREs Comput. Mol. Sci.* **2011**, *1*, 211–228. [[CrossRef](#)]
86. Grimme, S.; Antony, J.; Ehrlich, S.; Krieg, H. A consistent and accurate ab initio parametrization of density functional dispersion correction (DFT-D) for the 94 elements H–Pu. *J. Chem. Phys.* **2010**, *132*, 154104. [[CrossRef](#)]
87. Caldeweyher, E.; Ehlert, S.; Hansen, A.; Neugebauer, H.; Spicher, S.; Bannwarth, C.; Grimme, S. A generally applicable atomic-charge dependent London dispersion correction. *J. Chem. Phys.* **2019**, *150*, 154122. [[CrossRef](#)]
88. Naka, K.; Sato, H.; Higashi, M. Theoretical study of the mechanism of the solvent dependency of ESIPT in HBT. *Phys. Chem. Chem. Phys.* **2021** [[CrossRef](#)] [[PubMed](#)]
89. Laner, J.N.; Silva Junior, H.D.C.; Rodembusch, F.S.; Moreira, E.C. New insights on the ESIPT process based on solid-state data and state-of-the-art computational methods. *Phys. Chem. Chem. Phys.* **2021**, *23*, 1146–1155. [[CrossRef](#)] [[PubMed](#)]
90. Li, Y.; Siddique, F.; Aquino, A.J.A.; Lischka, H. Molecular dynamics simulation of the excited-state proton transfer mechanism in 3-hydroxyflavone using explicit hydration models. *J. Phys. Chem. A* **2021**, *125*, 5765–5778. [[CrossRef](#)]
91. Dunning, T.H. Gaussian basis sets for use in correlated molecular calculations. I. The atoms boron through neon and hydrogen. *J. Chem. Phys.* **1989**, *90*, 1007–1023. [[CrossRef](#)]
92. Self-consistent molecular orbital methods. XX. A basis set for correlated wave functions. *J. Chem. Phys.* **1980**, *72*, 650–654. [[CrossRef](#)]
93. Laurent, A.D.; Blondel, A.; Jacquemin, D. Choosing an atomic basis set for TD-DFT, SOPPA, ADC(2), CIS(D), CC2 and EOM-CCSD calculations of low-lying excited states of organic dyes. *Theor. Chem. Acc.* **2015**, *134*, 76. [[CrossRef](#)]
94. Sinnecker, S.; Rajendran, A.; Klamt, A.; Diedenhofen, M.; Neese, F. Calculation of solvent shifts on electronic g-tensors with the conductor-like screening model (COSMO) and its self-consistent generalization to real solvents (direct COSMO-RS). *J. Phys. Chem. A* **2006**, *110*, 2235–2245. [[CrossRef](#)]
95. Yang, Y.; Zhao, J.; Li, Y. Theoretical study of the ESIPT process for a new natural product quercetin. *Sci. Rep.* **2016**, *6*, 32152. [[CrossRef](#)]
96. Scalmani, G.; Frisch, M.J.; Mennucci, B.; Tomasi, J.; Cammi, R.; Barone, V. Geometries and properties of excited states in the gas phase and in solution: Theory and application of a time-dependent density functional theory polarizable continuum model. *J. Chem. Phys.* **2006**, *124*, 094107. [[CrossRef](#)] [[PubMed](#)]
97. Corni, S.; Cammi, R.; Mennucci, B.; Tomasi, J. Electronic excitation energies of molecules in solution within continuum solvation models: Investigating the discrepancy between state-specific and linear-response methods. *J. Chem. Phys.* **2005**, *123*, 134512. [[CrossRef](#)]
98. Marenich, A.V.; Cramer, C.J.; Truhlar, D.G. Universal solvation model based on solute electron density and on a continuum model of the solvent defined by the bulk dielectric constant and atomic surface tensions. *J. Phys. Chem. B* **2009**, *113*, 6378–6396. [[CrossRef](#)] [[PubMed](#)]
99. Cammi, R.; Tomasi, J. Remarks on the use of the apparent surface charges (ASC) methods in solvation problems: Iterative versus matrix-inversion procedures and the renormalization of the apparent charges. *J. Comput. Chem.* **1995**, *16*, 1449–1458. [[CrossRef](#)]
100. Cancès, E.; Mennucci, B.; Tomasi, J. A new integral equation formalism for the polarizable continuum model: Theoretical background and applications to isotropic and anisotropic dielectrics. *J. Chem. Phys.* **1997**, *107*, 3032–3041. [[CrossRef](#)]
101. Mennucci, B.; Cancès, E.; Tomasi, J. Evaluation of solvent effects in isotropic and anisotropic dielectrics and in ionic solutions with a unified integral equation method: Theoretical bases, computational implementation, and numerical applications. *J. Phys. Chem. B* **1997**, *101*, 10506–10517. [[CrossRef](#)]
102. Yuan, H.; Guo, X.; Zhang, J. Ab initio insights into the mechanism of excited-state intramolecular proton transfer triggered by the second excited singlet state of a fluorescent dye: An anti-Kasha behavior. *Mater. Chem. Front.* **2019**, *3*, 1225–1230. [[CrossRef](#)]
103. Caricato, M.; Mennucci, B.; Tomasi, J.; Ingrosso, F.; Cammi, R.; Corni, S.; Scalmani, G. Formation and relaxation of excited states in solution: A new time dependent polarizable continuum model based on time dependent density functional theory. *J. Chem. Phys.* **2006**, *124*, 124520. [[CrossRef](#)] [[PubMed](#)]
104. Marenich, A.V.; Cramer, C.J.; Truhlar, D.G.; Guido, C.A.; Mennucci, B.; Scalmani, G.; Frisch, M.J. Practical computation of electronic excitation in solution: Vertical excitation model. *Chem. Sci.* **2011**, *2*, 2143. [[CrossRef](#)]
105. Guido, C.A.; Scalmani, G.; Mennucci, B.; Jacquemin, D. Excited state gradients for a state-specific continuum solvation approach: The vertical excitation model within a Lagrangian TDDFT formulation. *J. Chem. Phys.* **2017**, *146*, 204106. [[CrossRef](#)]

106. Peng, Y.; Ye, Y.; Xiu, X.; Sun, S. Mechanism of Excited-State Intramolecular Proton Transfer for 1,2-Dihydroxyanthraquinone: Effect of Water on the ESIPT. *J. Phys. Chem. A* **2017**, *121*, 5625–5634. [[CrossRef](#)]
107. Crespo-Otero, R.; Barbatti, M. Recent advances and perspectives on nonadiabatic mixed quantum-classical dynamics. *Chem. Rev.* **2018**, *118*, 7026–7068. [[CrossRef](#)]
108. Tully, J.C. Molecular dynamics with electronic transitions. *J. Chem. Phys.* **1990**, *93*, 1061. [[CrossRef](#)]
109. Tully, J.C. Mixed quantum-classical dynamics. *Faraday Discuss.* **1998**, *110*, 407–419. [[CrossRef](#)]
110. Barbatti, M. Nonadiabatic dynamics with trajectory surface hopping method. *WIREs Comput. Mol. Sci.* **2011**, *1*, 620–633. [[CrossRef](#)]
111. Yarkony, D.R. Nonadiabatic quantum chemistry—Past, present, and future. *Chem. Rev.* **2012**, *112*, 481–498. [[CrossRef](#)] [[PubMed](#)]
112. Ben-Nun, M.; Quenneville, J.; Martínez, T.J. Ab initio multiple spawning: Photochemistry from first principles quantum molecular dynamics. *J. Phys. Chem. A* **2000**, *104*, 5161–5175. [[CrossRef](#)]
113. Curchod, B.F.E.; Martínez, T.J. Ab initio nonadiabatic quantum molecular dynamics. *Chem. Rev.* **2018**, *118*, 3305–3336. [[CrossRef](#)]
114. Zhao, L.; Wildman, A.; Tao, Z.; Schneider, P.; Hammes-Schiffer, S.; Li, X. Nuclear-electronic orbital Ehrenfest dynamics. *J. Chem. Phys.* **2020**, *153*, 224111. [[CrossRef](#)] [[PubMed](#)]
115. Belyaev, A.K.; Lasser, C.; Trigila, G. Landau-Zener type surface hopping algorithms. *J. Chem. Phys.* **2014**, *140*, 224108. [[CrossRef](#)]
116. Suchan, J.; Janoš, J.; Slaviček, P. Pragmatic approach to photodynamics: mixed Landau-Zener surface hopping with intersystem crossing. *J. Chem. Theory Comput.* **2020**, *16*, 5809–5820. [[CrossRef](#)]
117. Pratihari, S.; Ma, X.; Homayoon, Z.; Barnes, G.L.; Hase, W.L. Direct chemical dynamics simulations. *JACS* **2017**, *139*, 3570–3590. [[CrossRef](#)]
118. Barbatti, M.; Granucci, G.; Persico, M.; Ruckebauer, M.; Vazdar, M.; Eckert-Maksić, M.; Lischka, H. The on-the-fly surface-hopping program system Newton-X: Application to ab initio simulation of the nonadiabatic photodynamics of benchmark systems. *J. Photochem. Photobiol. A* **2007**, *190*, 228–240. [[CrossRef](#)]
119. Barbatti, M.; Ruckebauer, M.; Plasser, F.; Pittner, J.; Granucci, G.; Persico, M.; Lischka, H. Newton-X: A surface-hopping program for nonadiabatic molecular dynamics. *WIREs Comput. Mol. Sci.* **2014**, *4*, 26–33. [[CrossRef](#)]
120. Richter, M.; Marquetand, P.; González-Vázquez, J.; Sola, I.; González, L. SHARC: Ab initio molecular dynamics with surface hopping in the adiabatic representation including arbitrary couplings. *J. Chem. Theory Comput.* **2011**, *7*, 1253–1258. [[CrossRef](#)] [[PubMed](#)]
121. Du, L.; Lan, Z. An on-the-fly surface-hopping program JADE for nonadiabatic molecular dynamics of polyatomic systems: Implementation and applications. *J. Chem. Theory Comput.* **2015**, *11*, 1360–1374. [[CrossRef](#)] [[PubMed](#)]
122. Understanding the surface hopping view of electronic transitions and decoherence. *Annu. Rev. Phys. Chem.* **2016**, *67*, 387–417. [[CrossRef](#)] [[PubMed](#)]
123. Tuna, D.; Spörkel, L.; Barbatti, M.; Thiel, W. Nonadiabatic dynamics simulations of photoexcited urocanic acid. *Chem. Phys.* **2018**, *515*, 521–534. [[CrossRef](#)]
124. Xia, S.H.; Che, M.; Liu, Y.; Zhang, Y.; Cui, G. Photochemical mechanism of 1,5-benzodiazepin-2-one: Electronic structure calculations and nonadiabatic surface-hopping dynamics simulations. *Phys. Chem. Chem. Phys.* **2019**, *21*, 10086–10094. [[CrossRef](#)] [[PubMed](#)]
125. Ben-Nun, M.; Martínez, T.J. Ab initio quantum molecular dynamics. In *Advances in Chemical Physics*; John Wiley & Sons, Ltd.: Hoboken, NJ, USA, 2002; pp. 439–512. [[CrossRef](#)]
126. Leticia, G.; Roland, L. *Quantum Chemistry and Dynamics of Excited States: Methods and Applications*; Wiley: Hoboken, NJ, USA, 2021.
127. Fedorov, D.A.; Pruitt, S.R.; Keipert, K.; Gordon, M.S.; Varganov, S.A. Ab initio multiple spawning method for intersystem crossing dynamics: Spin-forbidden transitions between 3B1 and 1A1 States of GeH2. *J. Phys. Chem. A* **2016**, *120*, 2911–2919. [[CrossRef](#)]
128. Barca, G.M.J.; Bertoni, C.; Carrington, L.; Datta, D.; De Silva, N.; Deustua, J.E.; Fedorov, D.G.; Gour, J.R.; Gunina, A.O.; Guidez, E.; et al. Recent developments in the general atomic and molecular electronic structure system. *J. Chem. Phys.* **2020**, *152*, 154102. [[CrossRef](#)]
129. Levine, B.G.; Coe, J.D.; Virshup, A.M.; Martínez, T.J. Implementation of ab initio multiple spawning in the Molpro quantum chemistry package. *Chem. Phys.* **2008**, *347*, 3–16. [[CrossRef](#)]
130. Werner, H.J.; Knowles, P.J.; Knizia, G.; Manby, F.R.; Schütz, M. Molpro: A general-purpose quantum chemistry program package. *WIREs Comput. Mol. Sci.* **2012**, *2*, 242–253. [[CrossRef](#)]
131. Granucci, G.; Persico, M.; Toniolo, A. Direct semiclassical simulation of photochemical processes with semiempirical wave functions. *J. Chem. Phys.* **2001**, *114*, 10608–10615. [[CrossRef](#)]
132. Stewart, J. MOPAC: A semiempirical molecular orbital program. *J. Comput. Aided* **1990**, *4*, 1–103. [[CrossRef](#)] [[PubMed](#)]
133. Pijeu, S.; Foster, D.; Hohenstein, E.G. Effect of nonplanarity on excited-state proton transfer and internal conversion in salicylideneaniline. *J. Phys. Chem. A* **2018**, *122*, 5555–5562. [[CrossRef](#)] [[PubMed](#)]
134. Pijeu, S.; Foster, D.; Hohenstein, E.G. Excited-state dynamics of 2-(2'-hydroxyphenyl)benzothiazole: Ultrafast proton transfer and internal conversion. *J. Phys. Chem. A* **2017**, *121*, 4595–4605. [[CrossRef](#)] [[PubMed](#)]
135. Zhao, L.; Wildman, A.; Pavošević, F.; Tully, J.C.; Hammes-Schiffer, S.; Li, X. Excited state intramolecular proton transfer with nuclear-electronic orbital Ehrenfest dynamics. *J. Phys. Chem. Lett.* **2021**, *12*, 3497–3502. [[CrossRef](#)]
136. Webb, S.P.; Jordanov, T.; Hammes-Schiffer, S. Multiconfigurational nuclear-electronic orbital approach: Incorporation of nuclear quantum effects in electronic structure calculations. *J. Chem. Phys.* **2002**, *117*, 4106–4118. [[CrossRef](#)]

137. Li, X.; Tully, J.C.; Schlegel, H.B.; Frisch, M.J. Ab initio Ehrenfest dynamics. *J. Chem. Phys.* **2005**, *123*, 084106. [[CrossRef](#)]
138. Wang, L.; Prezhdo, O.V. A simple solution to the trivial crossing problem in surface hopping. *J. Phys. Chem. Lett.* **2014**, *5*, 713–719. [[CrossRef](#)]
139. Sun, Z.; Li, S.; Xie, S.; An, Z. Solution for the trivial crossing problem in surface hopping simulations by the classification on excited states. *J. Phys. Chem. C* **2018**, *122*, 8058–8064. [[CrossRef](#)]
140. Qiu, J.; Bai, X.; Wang, L. Crossing classified and corrected fewest switches surface hopping. *J. Phys. Chem. Lett.* **2018**, *9*, 4319–4325. [[CrossRef](#)] [[PubMed](#)]
141. Beck, M.; Jäckle, A.; Worth, G.A.; Meyer, H.D. The multiconfiguration time-dependent Hartree (MCTDH) method: A highly efficient algorithm for propagating wavepackets. *Phys. Rep.* **2000**, *324*, 1–105. [[CrossRef](#)]
142. Cederbaum, L.S.; Köppel, H.; Domcke, W. Multimode vibronic coupling effects in molecules. *Int. J. Quantum Chem.* **1981**, *15*, 251–267. [[CrossRef](#)]
143. Cederbaum, L.S. The multistate vibronic coupling problem. *J. Chem. Phys.* **1983**, *78*, 5714–5728. [[CrossRef](#)]
144. Worth, G.A.; Meyer, H.D.; Köppel, H.; Cederbaum, L.S.; Burghardt, I. Using the MCTDH wavepacket propagation method to describe multimode non-adiabatic dynamics. *Int. Rev. Phys. Chem.* **2008**, *27*, 569–606. [[CrossRef](#)]
145. Vendrell, O.; Meyer, H.D. Multilayer multiconfiguration time-dependent Hartree method: Implementation and applications to a Henon–Heiles Hamiltonian and to pyrazine. *J. Chem. Phys.* **2011**, *134*, 044135. [[CrossRef](#)]
146. Worth, G.A.; Beck, M.H.; Jäckle, A.; Meyer, H.D. *The Heidelberg MCTDH Package*; University of Heidelberg: Heidelberg, Germany, 2000.
147. Worth, G.A.; Giri, K.; Richings, G.W.; Burghardt, I.; Beck, M.H.; Jäckle, A.; Meyer, H.D. *The QUANTICS Package*; University of Birmingham: Birmingham, UK, 2015.
148. Perveaux, A.; Lorphelin, M.; Lasorne, B.; Lauvergnat, D. Fast and slow excited-state intramolecular proton transfer in 3-hydroxychromone: A two-state story? *Phys. Chem. Chem. Phys.* **2017**, *19*, 6579–6593. [[CrossRef](#)]
149. Anand, N.; Isukapalli, S.V.K.; Vennapusa, S.R. Excited-state intramolecular proton transfer driven by conical intersection in hydroxychromones. *J. Comput. Chem.* **2020**, *41*, 1068–1080. [[CrossRef](#)]
150. Anand, N.; Welke, K.; Irle, S.; Vennapusa, S.R. Nonadiabatic excited-state intramolecular proton transfer in 3-hydroxyflavone: S 2 state involvement via multi-mode effect. *J. Chem. Phys.* **2019**, *151*, 214304. [[CrossRef](#)]
151. Anand, N.; Nag, P.; Kanaparthi, R.K.; Vennapusa, S.R. O-H vibrational motions promote sub-50 fs nonadiabatic dynamics in 3-hydroxypyran-4-one: Interplay between internal conversion and ESIPT. *Phys. Chem. Chem. Phys.* **2020**, *22*, 8745–8756. [[CrossRef](#)]
152. Cao, Y.; Eng, J.; Penfold, T.J. Excited state intramolecular proton transfer dynamics for triplet harvesting in organic molecules. *J. Phys. Chem. A* **2019**, *123*, 2640–2649. [[CrossRef](#)] [[PubMed](#)]
153. Richings, G.W.; Robertson, C.; Habershon, S. Can we use on-the-fly quantum simulations to connect molecular structure and sunscreen action? *Faraday Discuss.* **2019**, *216*, 476–493. [[CrossRef](#)] [[PubMed](#)]
154. Westermayr, J.; Marquetand, P. Machine learning and excited-state molecular dynamics. *MLST* **2020**, *1*, 043001. [[CrossRef](#)]
155. Westermayr, J.; Gastegger, M.; Marquetand, P. Combining SchNet and SHARC: The SchNarc machine learning approach for excited-state dynamics. *J. Phys. Chem. Lett.* **2020**, *11*, 3828–3834. [[CrossRef](#)]